

Cross section of $\gamma\gamma \rightarrow \pi^+\pi^-\pi^0$ in chiral perturbation theory

J.W. Bos*, Y.C. Lin, and H.H. Shih
Department of Physics, National Central University
Chung Li, Taiwan 32054

NCUHEP 94-04

Abstract

We give the amplitude for $\gamma\gamma \rightarrow \pi^+\pi^-\pi^0$ in leading order chiral perturbation theory. For the case of real photons we calculate the total and differential cross section. Furthermore, we give the dependence of the total cross section on the invariant mass of one of the photons.

Chiral perturbation theory (ChPT) [1, 2, 3] has proven to be an useful method to describe reactions involving low-energy mesons. The method is closely related to QCD, and therefore comparison of ChPT predictions with experimental data provides an indirect test for QCD. Reactions that are particularly useful for this purpose are inelastic two photon processes. These type of reactions attracted a lot of experimental attention recently. In this letter we calculate the cross section for the specific channel $\gamma\gamma \rightarrow \pi^+\pi^-\pi^0$ in leading order ChPT. In contrast to the $\gamma\gamma \rightarrow \pi^+\pi^-$ channel this channel is sensitive to the *anomalous* or *odd intrinsic parity* sector of QCD.

In the ChPT approach (we need to consider here the meson sector only), one starts from the most general gauge invariant effective lagrangian in terms of meson degrees of freedom, which reflects the approximate chiral $SU(3)_L \times SU(3)_R$ symmetry of the QCD lagrangian. Based on this effective

*e-mail jwb@joule.phy.ncu.edu.tw

lagrangian a perturbation scheme is developed in which one expands in a systematic way in the external momenta and the meson masses. The leading terms in the expansion of an amplitude in these variables are given by the tree-level diagrams with vertices from the leading order lagrangian. Loop diagrams, and tree-level diagrams containing vertices from the next to leading order lagrangian, are suppressed by a power $(p/\Lambda_\chi)^2$ where p denotes the four momenta or mass of the mesons, and Λ_χ is the scale in the energy expansion, $\Lambda_\chi \approx 1$ GeV. At low energies, and since the meson masses are small compared to Λ_χ , one needs to keep only the first terms in this expansion. We will here only consider the amplitude in leading order, i.e. the tree-level.

The general ChPT lagrangian in the meson sector can be divided into an *even* and an *odd* intrinsic parity part [4]. The first consists of interactions among only an even number of mesons while the second consists of interactions among only an odd number of mesons. The effective lagrangian of ChPT in the odd intrinsic parity sector reads

$$\mathcal{L}_{\text{odd}} = \mathcal{L}_{\text{odd}}^{(4)} + \mathcal{L}_{\text{odd}}^{(6)} + \dots, \quad (1)$$

where the superscripts denote the momentum dimension. The leading term in eq. (1), $\mathcal{L}_{\text{odd}}^{(4)}$, is the well-known anomalous Wess-Zumino-Witten term [4, 5]. For our application it is sufficient to take

$$\begin{aligned} \mathcal{L}_{\text{odd}}^{(4)} = & -\frac{iN_c e}{48\pi^2} \epsilon^{\mu\nu\alpha\beta} A_\mu \text{Tr} \left[Q(\partial_\nu \Sigma \partial_\alpha \Sigma^\dagger \partial_\beta \Sigma \Sigma^\dagger - \partial_\nu \Sigma^\dagger \partial_\alpha \Sigma \partial_\beta \Sigma^\dagger \Sigma) \right] \\ & - \frac{iN_c e^2}{24\pi^2} \epsilon^{\mu\nu\alpha\beta} (\partial_\mu A_\nu) A_\alpha \text{Tr} \left[Q^2 \partial_\beta \Sigma \Sigma^\dagger + Q^2 \Sigma^\dagger \partial_\beta \Sigma \right. \\ & \left. + \frac{1}{2} Q \Sigma Q \Sigma^\dagger \partial_\beta \Sigma \Sigma^\dagger - \frac{1}{2} Q \Sigma^\dagger Q \Sigma \partial_\beta \Sigma^\dagger \Sigma \right]. \end{aligned} \quad (2)$$

The meson fields are contained in the SU(3) matrix Σ given by

$$\Sigma = \exp(2i\pi/f_\pi), \quad (3)$$

where

$$\pi = \frac{1}{\sqrt{2}} \begin{pmatrix} \frac{1}{\sqrt{2}}\pi^0 + \frac{1}{\sqrt{6}}\eta & \pi^+ & K^+ \\ \pi^- & -\frac{1}{\sqrt{2}}\pi^0 + \frac{1}{\sqrt{6}}\eta & K^0 \\ K^- & \bar{K}^0 & -\frac{2}{\sqrt{6}}\eta \end{pmatrix} \quad (4)$$

and f_π is the pion decay constant, $f_\pi = 94$ MeV. In eq. (2) A_μ is the electromagnetic field and Q is the charge operator in flavor space given by

$$Q = \text{diag}(2/3, -1/3, -1/3). \quad (5)$$

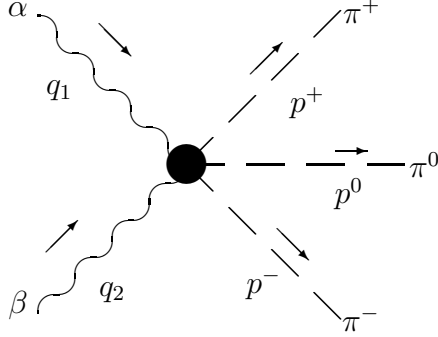


Figure 1: *Kinematics of the $\gamma\gamma \rightarrow \pi^+\pi^-\pi^0$ process*

The second term in the lagrangian eq. (1), $\mathcal{L}_{\text{odd}}^{(6)}$, is of higher order in the momentum and mass expansion [6] and therefore omitted in this leading order calculation.

The effective lagrangian in the even intrinsic parity sector of ChPT is, to leading order, given by

$$\mathcal{L}_{\text{even}}^{(2)} = \frac{f_\pi}{4} \text{Tr}(D_\mu \Sigma D^\mu \Sigma^\dagger + \chi \Sigma^\dagger + \Sigma \chi^\dagger), \quad (6)$$

where the covariant derivative, D_μ , is defined by

$$D_\mu \Sigma = \partial_\mu \Sigma + ie A_\mu (Q \Sigma - \Sigma Q) \quad (7)$$

and χ is the chiral symmetry breaking mass matrix,

$$\chi = B \text{diag}(m_u, m_d, m_s). \quad (8)$$

We now turn to the reaction $\gamma\gamma \rightarrow \pi^+\pi^-\pi^0$ using the lagrangian eq. (2) and eq. (6). In fig. 1 we define our notation for the external momenta, and the Feynman diagrams contributing to the leading order amplitude are shown in fig. 2. The pole diagrams (a) and (b) in fig. 2 consist of one vertex from the odd intrinsic parity lagrangian $\mathcal{L}_{\text{odd}}^{(4)}$ and one from the normal intrinsic parity lagrangian $\mathcal{L}_{\text{even}}^{(2)}$, while diagram (c) consist only of one vertex from $\mathcal{L}_{\text{odd}}^{(4)}$. Since the $\eta\pi^+\pi^-\pi^0$ coupling is an isospin breaking effect, diagram (b) with an intermediate η propagator is suppressed.

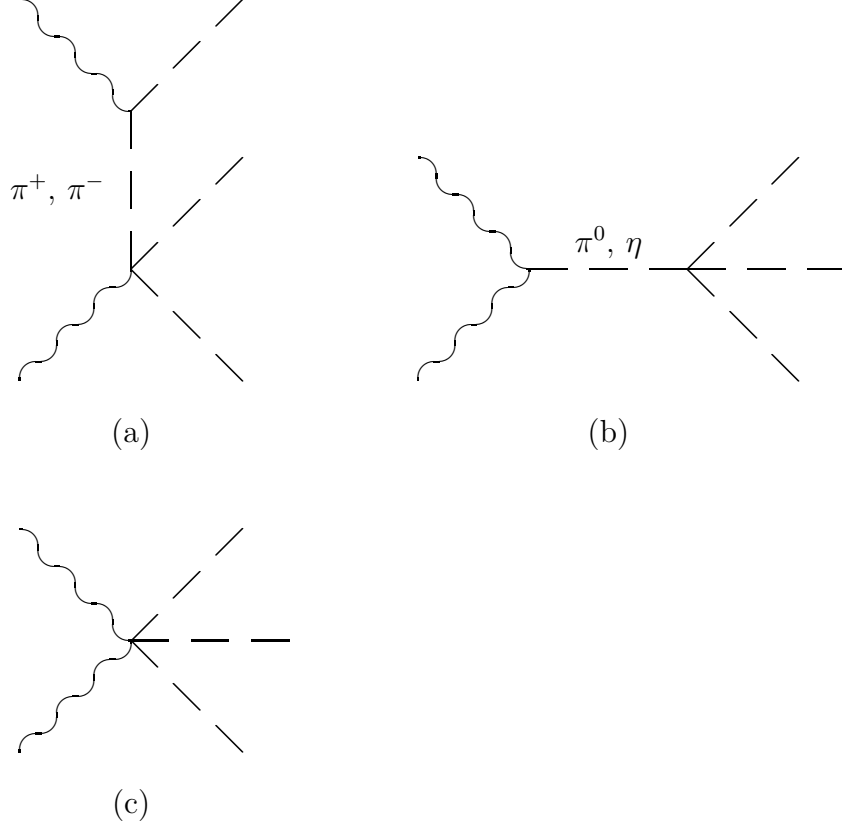


Figure 2: *Leading order Feynman diagrams for $\gamma\gamma \rightarrow \pi^+\pi^-\pi^0$.*

Applying the standard Feynman rules and averaging over the polarizations of the initial photons the amplitude squared reads

$$|\mathcal{M}|^2 = \frac{1}{4}\Gamma_{\alpha\beta}\Gamma^{\alpha\beta}, \quad (9)$$

where

$$\begin{aligned} \Gamma^{\alpha\beta} = & \frac{ie^2 N_c}{12\pi^2 f_\pi^3} \left[\epsilon^{\alpha\beta\mu\nu} q_{1\mu} q_{2\nu} \left(\frac{(p^+ + p^-)^2 - m_\pi^2}{(q_1 + q_2)^2 - m_\pi^2} - \frac{1}{3} \right) \right. \\ & + \epsilon^{\alpha\beta\mu\nu} \left(\frac{4}{3} q_{1\mu} q_{2\nu} - (q_1 - q_2)_\mu (p^+ + p^-)_\nu \right) \\ & - \left[\epsilon^{\alpha\mu\nu\rho} \left(\frac{(2p^+ - q_2)^\beta}{q_2^2 - 2p^+ \cdot q_2} p_\mu^- q_{1\nu} (p^+ - q_2)_\rho \right) \right. \\ & \left. \left. + \frac{(2p^- - q_2)^\beta}{q_2^2 - 2p^- \cdot q_2} p_\mu^+ q_{1\nu} (p^- - q_2)_\rho \right) + (q_1 \leftrightarrow q_2, \alpha \leftrightarrow \beta) \right]. \quad (10) \end{aligned}$$

This is in agreement with the early result by Adler et al [7] using a current

algebra approach¹.

The differential cross section for $\gamma\gamma \rightarrow \pi^+\pi^-\pi^0$ is for real photons given by

$$d\sigma = \frac{1}{2E_{\text{cms}}} |\mathcal{M}|^2 \frac{d\vec{p}^+}{2E^+(2\pi)^3} \frac{d\vec{p}^0}{2E^0(2\pi)^3} \frac{d\vec{p}^-}{2E^-(2\pi)^3} (2\pi)^4 \delta^4(q_1 + q_2 - p^+ - p^0 - p^-), \quad (12)$$

where the momenta are the same as in fig. 1, and E_{cms} is the total center of mass energy of the two photons. The amplitude squared depends on five kinematical variables for which we choose the invariants

$$\begin{aligned} s &= (q_1 + q_2)^2; \quad s_1 = (p^+ + p^0)^2; \quad s_2 = (p^- + p^0)^2 \\ t_1 &= (q_1 - p^+)^2; \quad t_2 = (q_2 - p^-)^2. \end{aligned} \quad (13)$$

The total cross section, σ , as a function of $s = E_{\text{cms}}^2$, is given in terms of these invariants by

$$\sigma(s) = \frac{\pi}{32s^2(2\pi)^5} \int \frac{|\mathcal{M}|^2}{\sqrt{-\Delta_4}} dt_1 dt_2 ds_1 ds_2, \quad (14)$$

where $\Delta_4 = \Delta_4(s, s_1, s_2, t_1, t_2)$ is given by the determinant

$$\Delta_4 = \frac{1}{16} \det \begin{pmatrix} 2s_2 & s_2 - t_1 & s + s_2 - m_\pi^2 & s_2 \\ s_2 - t_1 & 0 & s & m_\pi^2 - t_2 \\ s + s_2 - m_\pi^2 & s & 2s & s - s_1 + m_\pi^2 \\ s_2 & m_\pi^2 - t_2 & s - s_1 + m_\pi^2 & 2m_\pi^2 \end{pmatrix}. \quad (15)$$

The range of the integration in eq. (14) is the physical region of the process, which satisfies $\Delta_4 \leq 0$ [8].

In fig. 3-a we show our prediction for the total cross section as a function of the total center of mass energy $E_{\text{cms}} = \sqrt{s}$, where we varied E_{cms} from threshold, $E_{\text{cms}} = 3m_\pi$ up to $E_{\text{cms}} = 0.7$ GeV. Of course, at and above this point contributions from resonances like the η and η' , and also loop diagrams are expected to be important. More essential features of the reaction

¹To arrive at eq. (10) one must take for F^π , $F^{3\pi}$, and x in Ref. [7]

$$F^\pi = \frac{\alpha}{\pi f_\pi}; \quad eF^{3\pi} = \frac{\alpha}{\pi f_\pi^3}; \quad x = 0. \quad (11)$$

Figure 3: (a) Total and (b) differential cross section for different values of s (units of GeV).

mechanism are contained in the differential cross sections. Fig. 2-b shows $d\sigma/ds_1$ as a function of the invariant mass of the final $\pi^+\pi^0$ system, $\sqrt{s_1}$, for different values of s . The range of $\sqrt{s_1}$ is determined by the available phase space. Because of charge conjugation invariance the differential cross section $d\sigma/ds_2$ has the same form as $d\sigma/ds_1$ and is therefore not shown here.

In a electron-positron collider, a measurement with two real photons requires double tagging of the final electron and positron at 0° (for discussion of experimental aspects of photon photon reactions see e.g. Ref. [9]). The detection efficiency is increased by allowing for virtual photons, $q_i^2 \neq 0$, as in a single tagging or no tagging experimental situation. With virtual photons eq. (14) for the total cross section becomes

$$\sigma(s) = \frac{\pi}{32\lambda(s, q_1^2, q_2^2)(2\pi)^5} \int \frac{|\mathcal{M}|^2}{\sqrt{-\Delta_4}} dt_1 dt_2 ds_1 ds_2, \quad (16)$$

where $\Delta_4 = \Delta_4(s, s_1, s_2, t_1, t_2, q_1^2, q_2^2)$ is given by the determinant

$$\Delta_4 = \frac{1}{16} \det \begin{pmatrix} 2s_2 & s_2 - t_1 + q_2^2 & s + s_2 - m_\pi^2 & s_2 \\ s_2 - t_1 + q_2^2 & 2q_2^2 & s - q_1^2 + q_2^2 & q_2^2 + m_\pi^2 - t_2 \\ s + s_2 - m_\pi^2 & s - q_1^2 + q_2^2 & 2s & s - s_1 + m_\pi^2 \\ s_2 & q_2^2 + m_\pi^2 - t_2 & s - s_1 + m_\pi^2 & 2m_\pi^2 \end{pmatrix} \quad (17)$$

and

$$\lambda(s, q_1^2, q_2^2) = (s - q_1^2 - q_2^2) - 4q_1^2 q_2^2. \quad (18)$$

Here we will consider the situation of a single tagging experiment, i.e. only one of the initial photons is real, $q_1^2 = 0$, while the other is virtual, $q_2^2 \neq 0$. The dependence of the total cross section on the virtual photon mass $W_q = \sqrt{q_2^2}$, with $q_1^2 = 0$, is shown in fig. 4. Again, the different curves correspond to different values of s . We varied W_q from $W_q = 0$ up to the $W_q = 2m_\pi$, the threshold for the production of two on-shell pions by the virtual photon. The dependence of the total cross section on W_q is moderate, only a variation

Figure 4: q^2 dependence of the total cross section for different values for s (units of GeV)

of about 10 % over the whole range of W_q . It indicates that compared to a double tagging situation the cross section in the experimentally more favorable single tagging situation is not much smaller in the kinematical range considered here.

The energy range for which the above calculation can be used depends on the magnitude of next-to-leading order corrections. This calculation is only valid in leading order in the $(p/\Lambda_\chi)^2$ expansion. In next to leading order ChPT not only chiral loops but also the *free* parameters from $\mathcal{L}_{\text{odd}}^{(6)}$ in eq. (1) enter the description. To give an estimate of higher order effect it is therefore necessary to determine these parameters, which usually cannot be done in a model independent way. However, comparing with similar two photon processes it has been shown that the width of π^0 decay into two photons is described very well by a leading order calculation [10, 11]. Since this process is sensitive to the same part of the ChPT lagrangian as $\gamma\gamma \rightarrow \pi^+\pi^-\pi^0$ we expect that also in the latter higher order correction are small. For virtual photons corrections to π^0 decay from $\mathcal{O}(p^6)$ terms have shown to be sizable [12], and we therefore expect that this goes through for photon photon collisions involving virtual photons. A detailed study of the importance of higher order effects is currently in progress.

References

- [1] L.-F. Li and H. Pagels, Phys. Rev. Lett. **26**, 1204 (1971).
- [2] S. Weinberg, Physica **96A**, 327 (1979).
- [3] J. Gasser and H. Leutwyler, Annals of Physics **150**, 142 (1984).
- [4] E. Witten, Nucl. Phys. **B223**, 422 (1983).
- [5] J. Wess and B. Zumino, Phys. Lett. **B37**, 95 (1971).

- [6] J. Bijnens, Nucl. Phys. **B367**, 709 (1991).
- [7] S. Adler, B. Lee, and S. Treiman, Phys. Rev. **D4**, 3497 (1971).
- [8] E. Byckling and K. Kajantie, in *Particle kinematics* (Wiley, New York, 1973), Chap. 5.
- [9] C. Berger and W. Wagner, Phys. Rep. **146**, 1 (1987).
- [10] J. Donoghue, B. Holstein, and Y. Lin, Phys. Rev. Lett. **55**, 2766 (1985).
- [11] J. Donoghue and D. Wyler, Nucl. Phys. **B316**, 289 (1989).
- [12] J. Bijnens, Int. Journ. Mod. Phys. **A8**, 3045 (1993).

This figure "fig1-1.png" is available in "png" format from:

<http://arxiv.org/ps/hep-ph/9407216v1>

This figure "fig1-2.png" is available in "png" format from:

<http://arxiv.org/ps/hep-ph/9407216v1>

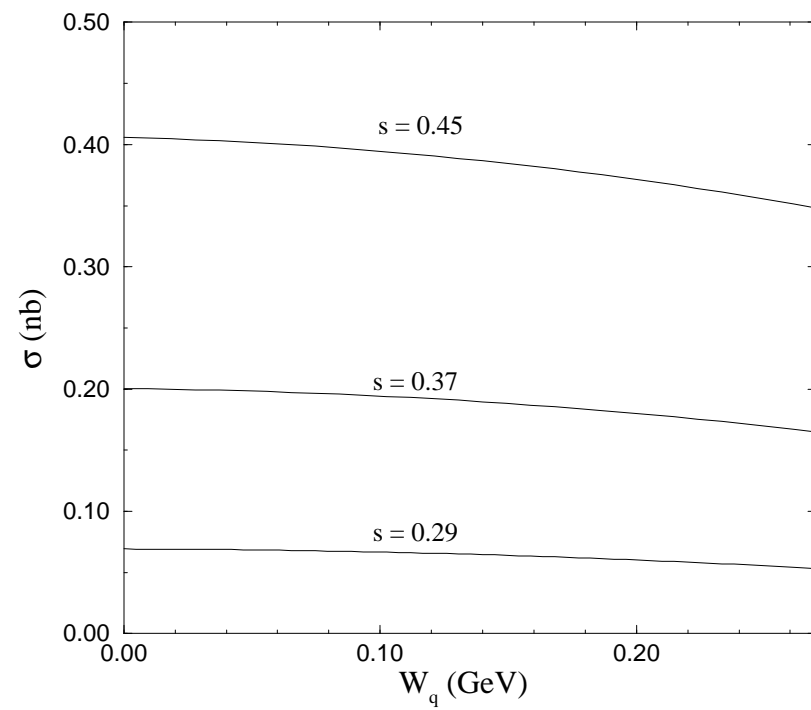
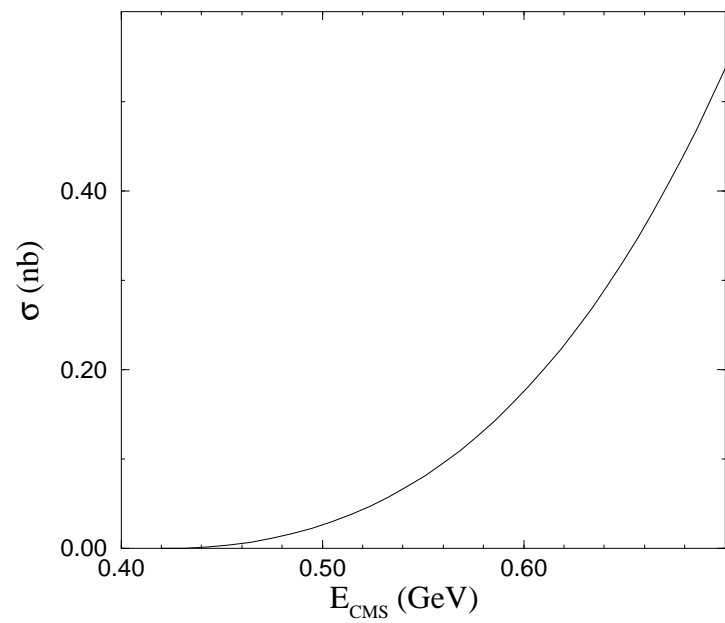
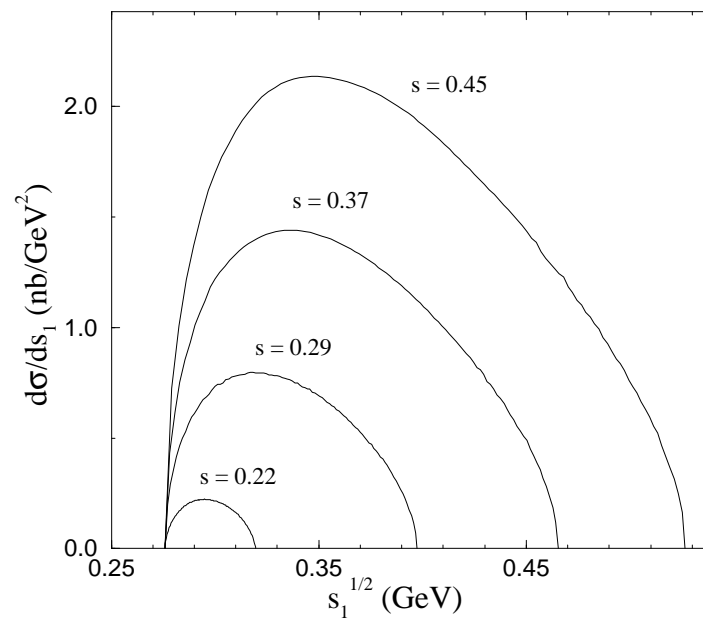


Fig . 4



(a)



(b)

Fig . 3